THE BALTIC JOURNAL
OF ROAD AND BRIDGE ENGINEERING

ISSN 1822-427X / eISSN 1822-4288
2017 Volume 12(1): 1–11

THE ROLE OF BACKFILL QUALITY ON CORRUGATED STEEL PLATE CULVERT BEHAVIOUR

Damian Beben

Dept of Geotechnics and Geodesy, Opole University of Technology, Katowicka 48, 45-061 Opole, Poland
E-mail: d.beben@po.opole.pl

Abstract. The subject of the article is a three-dimensional numerical analysis of the impact of backfill quality on the deformation of corrugated steel plate culvert. In the numerical analysis, the author took into consideration three different backfill types. The paper presents the calculations performed with the use of Abaqus program based on finite element method. A steel shell was modelled with the use of the theory of orthotropic plates, and backfill with the use of elastic-perfectly plastic Drucker-Prager model. The author made the numerical calculations under static live loads for the corrugated steel plate culvert with a span of 12.315 m and height of shell of 3.555 m. Soil cover over the shell crown was equal to 1.0 m. The steel shell consisted of the sheets of the corrugation of 0.14×0.38 m and plate thickness of 0.0071 m. The main aim of this paper is to present the impact of backfill quality (internal friction angle, unit weight, Young's modulus) on the effort of the steel shell. The paper also shows the numerical calculations for the actual culvert, which previously had been studied experimentally. The author compared the obtained numerical results to the results of experiments. Parametric analysis showed that the angle of internal friction was a major factor in corrugated steel plate culverts. Considering the entire width of the corrugated steel plate culvert, the calculation model II was most favourable. The proposed method of modelling of the corrugated steel plate culvert allowed obtaining reasonable values of displacements and stresses in comparison to experimental results.

Keywords: backfill, culverts, displacement, finite element analysis, static loads, stress.

1. Introduction

Structures from corrugated steel plates (CSP) have recently gained popularity in the transport engineering as an alternative to conventional bridge solutions. Some authors call these structures as the soil-steel bridges (Pettersson *et al.* 2015). The main reasons for usage of these structures are relatively low costs and short construction period (Janusz, Madaj 2009). The bearing element of these structures is the soil-steel composite system which uses arching of the load in soil and interaction between flexible steel shell and backfill (Machelski 2008).

Backfill is the key element in these structural solutions. Therefore, the author decided to analyse the impact of the chosen backfill parameters on deformations (displacement and stresses) of the CSP culvert. Selection of soil (backfill), which has proper characteristics and its appropriate arrangement and compaction play a fundamental role in the achievement of required load carrying capacity of that type of culverts. In general, the used soil should be water-permeable, free from grittiness and frozen ground, with uneven graining, well compactable, non-aggressive, and free of organic elements. Depending on the selected height of the corrugation it is recommended that the size of grains would not exceed:

(i) 32 mm (for corrugation 100×20 mm),
(ii) 42 mm (150×50 and 200×55 mm) and
(iii) 120 mm (380×140 mm) (Janusz, Madaj 2009).

The important parameter of backfill is the angle of internal friction. It depends on a type of soil and compaction degree. For correctly compacted backfill (compaction degree Is = 0.95–1.00) the angle of internal friction is within the range of 36°–45°. There is a relation that the higher the angle of internal friction, the higher the soil shear strength, which directly affects the rise of the safety of these structural systems. Yeau, Sezen (2012) presented the new procedure of the load rating estimation for the CSP road culverts. The proposed method did not include a rating factor for the cover depth.

Experimental studies on CSP culverts under static (Flener 2009a, 2010; Elshimi *et al.* 2014; Kunecki 2006; Manko, Beben 2005; Sezen *et al.* 2008; Yeau *et al.* 2009) and dynamic live loads (Beben 2013a, 2013b, 2014; Flener, Karoumi 2009b; Mellat *et al.* 2014) were carried out repeatedly. Mai *et al.* (2014a) showed the latest analysis

doi:10.3846/bjrbe.2017.01

of the CSP culverts behaviour (intact culvert with well-compacted backfill) and a corroded culvert in loose backfill during backfilling and under imposed surface loads. Sheldon *et al.* (2015) presented the field performance of culvert joints in five existing pipe culverts under static and dynamic live loads. The results indicated that separation at the joint was quite significant at times. Simpson *et al.* (2015) presented a series of experimental laboratory tests of a deteriorated CSP culvert at two different burial depths (0.6 m and 0.9 m) under surface static loading before and after the culvert rehabilitation using a grouted high-density polyethylene.

Researchers conducted numerical analyses, and noticed many problems, mostly in the range of modelling of backfill and steel shell (Machelski 2008). Esmaeili *et al.* (2013) presented similar numerical analysis concerning the depth of soil cover. Sargand *et al.* (2008) presented the 2D numerical simulation of large-diameter pipe culvert using the CANDE-89 program. The received numerical predictions were unsatisfactory in comparison to experimental results. El-Taher (2009) analysed the effect of backfill erosion on the stability of the deteriorated metal culverts with using the elastic soil modulus variabilities. The elastic buckling analyses demonstrated that the development of backfill erosion causes substantial reductions in the factor of culvert safety. Katona (2010) presented a method of analysing and evaluating of buried culverts and cut-and-cover tunnels for seismic loading in addition to standard static loading from dead and live loads. Brachman *et al.* (2012) analysed a deep-corrugated steel box culvert without backfill. They modelled the box culvert using the corrugated structure (first model) and the orthotropic shell theory (second model). The corrugated analysis provided calculation values closer to those that were measured. Yeau *et al.* (2014) performed a two-dimensional (2D) and three-dimensional (3D) analyses of the impact of various parameters on the behaviour of 14 metal culverts under static load. The authors considered three different types of soil in 2D analysis and two-boundary backfill elastic modulus in the 3D analysis, respectively. The obtained calculated displacements from the 2D analysis were larger than measured ones. Moreover, they found that thrust forces did not undergo significant changes depending on the applied backfills. Mai *et al.* (2014b) presented the 2D finite element analysis for the deteriorated corrugated metal culverts with a span of 1.8 m. All the finite element models were unable to capture non-linear behaviour of the deteriorated culvert with poor backfill as well as the culverts at high surface loading due to the use of linear elastic models. Wadi *et al.* (2015) presented the numerical analysis of CSP culvert located in sloping terrain and considered the simulation of the soil loading effects. Beben, Stryczek (2016) presented a numerical modelling of a soil-steel bridge with reinforced concrete (RC) relieving slab. The obtained numerical results were overestimated in comparison to the site test results.

The calculation results obtained by use of the computational models as compared to the experimental data were insufficiently satisfactory. Therefore there is a need to conduct further numerical analyses of CSP culverts. Also, the role of backfill quality seems to be an essential element for the CSP culvert safety. Therefore, the researchers should conduct the analyses in that regard. Moreover until now, an efficient method for dimensioning of these structures has not been developed, despite the existence of many analytical methods, e.g. Sundquist-Petersson (Pettersson, Sundquist 2014), *CAN/CSA-S6-06 Canadian Highway Bridge Design Code* and *American Association State Highway and Transportation Officials LRFD Bridge Design Specifications*. However, they do not allow for accurate determination of internal forces in those bridge structures, and besides, have some limitations in the application, for example, the object span, depth of soil cover.

The aim of this paper was to present the influence of backfill quality (internal friction angle, unit weight, Young's modulus) on the effort of the shell in CSP culvert. The paper shows the numerical calculations for the actual CSP culvert. Manko, Beben (2005) examined this culvert experimentally. In present calculations the author used the Abaqus program based on FEM. Static live loads according to three various scenarios were applied during numerical analysis. The modelling of steel shell included the application of the theory of orthotropic plates. This approach resulted in a decrease in complexity of steel shell model because the main aim of this paper is to assess the influence of the backfill quality on the culvert deformations. The backfill modelling included with the use of elastic-perfectly plastic Drucker-Prager model. The author compared the obtained results to the results of experiments. Conclusions relate mainly to the evaluation of the impact of backfill quality on the effort of steel shell and giving parameters that are of utmost importance. Also, the author gave reasons for the differences in calculation and experimental results.

2. Short description of the CSP culvert

Analysed structure was a culvert composed of the shell with corrugated steel plate backfilled with soil. In the cross section, the analysed road culvert had a single shell span with an effective length of 12.315 m connected rigidly with a RC continuous footing (Fig. 1). The width of the culvert shell at the top was 12.915 m, and at the bottom was 20.574 m. Radiuses of curvature of shell were as follows R_c = 11.43 m for the crown and R_h = 1.016 m for haunches. In the plan view, the object lied perpendicularly to the river current, and the vertical rise of culvert shell amounted to 3.555 m. The shell was covered with the layers of water-permeable soil (about 0.20–0.30 m thick and graining of 10–32 mm) properly compacted (to reach compaction degree 0.95 for the soil connected directly with the steel structure and 0.98 for the remaining part of the backfill), allowing pavement to be laid on broken stone base. The thickness of the soil cover in the crown (backfill, road foundation, and asphalt) was equal to 1.0 m. The load bearing structure consisted of the sheets of corrugation of 0.14×0.38 m and plate thickness of 0.0071 m, connected using high strength bolts M20 (class 8.8) tightened with a twisting moment of 350–400 Nm. The culvert had designed to transfer loads by the *Bro 2004 Swedish Road Administration Design Standard for*

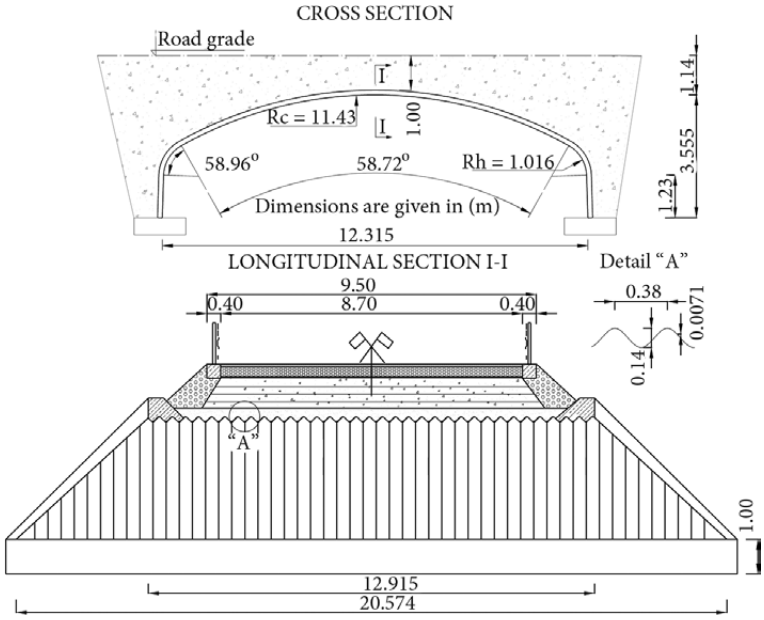

Fig. 1. CSP culvert

Bridges, what compared with the *PN-85/S–10030 1985 Polish Bridge Standard. Bridge Structures. Loads* correspond to a Class A (vehicle weight of 500 kN).

A strength of the used structural steel corresponded to that of Polish steel S315MC (the guaranteed yield strength of the steel used to manufacture corrugated plates was 314 MPa according to *PN-EN 10149-2:2014-02 Flat Products Hot Rolled with Steels on High Yield Strength for Cold Forming. Part 2: Technical Delivery Conditions for Thermomechanically Rolled Products*). Manko, Beben (2005) showed a detailed description of the culvert.

3. Numerical model description

3.1. General remarks

For computations of CSP culvert, the Abaqus/CEA ver. 6.11 was used, based on the FEM (Zienkiewicz, Taylor 2000). In the numerical model, the author made efforts to reflect the actual geometry of the analysed culvert, while not taking into account the secondary elements that may affect the increasing complexity of the model and considerably extended time for computation. Three numerical models of CSP culvert with different parameters of backfill were developed. Other parts of the culvert were all the same in each numerical models. Due to the compound shaped structure, the author simplified the numerical models slightly, although maintained the main parameters of the culvert (height and span of the steel shell, top shell length, various radiuses of the shell, and soil cover in shell crown). The model omitted elements, such as slopes, RC collars reinforcing inlet and outlet of the shell and guardrails. These items should not significantly affect the computational results, because they are located outside the range of actual loading, and at the same time represent only additional accessories of the culvert.

The author performed CSP culvert calculations under static live loads in 3D. Application of the incremental analysis – the Full Newton method allowed to consider the non-linearity in computational models. CSP culvert models were parts of the 3D space, which were in the dimensions of 16.32×9.50×4.70 m. Modelling the soils placed at a distance greater than 2 m from the steel shell did not substantially affected the obtained results of computations, while in this case, boundary conditions were rather decisive, which reflected the real structure. Hence, the modelling process did not include the RC foundations, as an element of rigid support for the structure.

The computational model constituted a finite element mesh in the shape of a cuboids C3D8R (solid elements) and tetrahedrons S4R (shell elements). In each calculation models, nodes had six degrees of freedom (U1, U2, U3 – displacement directions on the axes OX, OY, OZ, and UR1, UR2, UR3 – rotation directions relative to the axis OX, OY, OZ, respectively), wherein nodes of elements with their edges laying on external surfaces of the numerical model were blocked at all degrees of freedom – rotations and displacements (total restraint).

3.2. Material characteristics

3D shell tetrahedral elements (S4R) were used to model a steel shell. The author defined the remaining units (backfill and roadway layers) as elements with properties of a solid (C3DR8). The material parameters were chosen based on available technical data (the culvert elements and asphalt properties obtained from the producers of such materials and the backfill obtained from the project of this culvert) and material characteristics included in the Abaqus software, that were:

– CSP shell was modelled as a flat with appropriate parameters of the orthotropic shell (Fig. 2) using the following Eqs (1)–(4):

• equivalent thickness of plate:

$$t_{equ.} = \sqrt{12\frac{I}{A}}, \quad (1)$$

where I – moment of inertia (2.416e-8 m^4/m); A – cross-sectional area (9.81e-6 m^2/m);

• equivalent elastic modulus of the material (Young modulus) in the circumferential direction of culvert shell:

$$E_{x\ equ.} = 12\frac{EI}{t_{equ.}^3}, \quad (2)$$

where E – a Young modulus of steel structure assumed as 210 GPa;

• equivalent Young modulus in the longitudinal direction of the culvert shell:

$$E_{y\ equ.} = E\left(\frac{t}{t_{equ.}}\right)^3, \quad (3)$$

where t – a plate thickness (0.007 m);

• shear modulus for the corrugated steel plates was different in different directions. In this paper, an average value for the equivalent shear modulus was used based on the below Eq (4):

$$G_{equ.} = \frac{\sqrt{E_{x\ equ.}\ E_{y\ equ.}}}{2(1+\nu)}, \quad (4)$$

where ν – Poisson ratio (ν = 0.3).

Table 1 presents the equivalent parameters of corrugated plate used in the numerical analysis. The author defined the plate elements by shell-type elements (SR4) as an elastic-plastic material with a density γ = 78.5 kN/m^3 and yield strength σ = 314 MPa. In this case, adopted curvature control accuracy was 0.01 m, due to the complexity of shell itself and its curvilinear shape. The bolt connections between the steel plate elements were omitted during modelling. Parameters steel shell were the same in all analysed computational models.

– Backfill (medium size sand) with a thickness of 0.50 m (over the crown shell) was defined as elastic-plastic material (C3DR8 solid-type element) with the hyperbolic Drucker-Prager yield criterion with parameters presented in Table 2 for three numerical models. The elastic, perfectly plastic Drucker-Prager model is an approximation by a cone of the pyramid Coulomb-Mohr (Fig. 3). This approach resulted in higher numerical efficiency caused by eliminating kinks of plasticity surface. The cohesion and angle of internal friction were the most important parameters for the Drucker-Prager model. This paper showed the approximation as for the plane state of deformation. It

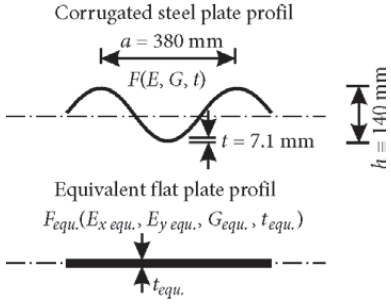

Fig. 2. Orthotropic characteristics of flat plates used in numerical model of shell

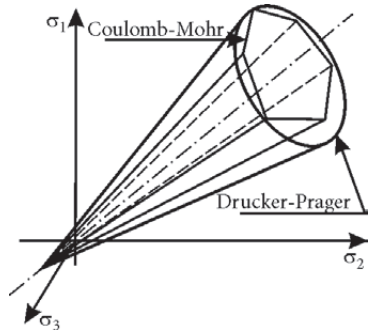

Fig. 3. Plasticity surfaces for Drucker-Prager model and Coulomb-Mohr model

Table 1. Orthotropic properties of the CSP culvert

Element	Equivalent thickness of plate	Equivalent Young modulus in direction:		Equivalent shear modulus
		circumferential	longitudinal	
	$t_{equ.}$, m	$E_{x\ equ.}$, GPa	$E_{y\ equ.}$, GPa	$G_{equ.}$, GPa
Shell structure	0.172	11.94	0.0142	0.158

Table 2. Variables of backfill parameters used for numerical calculation of CSP culvert

Numerical model	Angle of internal friction,	Unit weight,	Young modulus,	Compaction degree according to the *PN-EN 1997-2:2009. Eurocode 7: Geotechnical Design – Part 2: Ground Investigation and Testing*	Saturation degree
	o	kN/m^3	MPa		
I	45	19	80	0.90	moist
II	40	18	70	0.80	air-dry
III	35	21	90	0.98	wet

led to the identity-compliance of the results achieved with the Drucker-Prager model with similar results obtained by using the Coulomb-Mohr model regarding stability and limit load capacity. The Drucker-Prager model is most commonly used (similarly to the use of the Coulomb-Mohr model) with a non-associated flow law (dilatation angle $\alpha = 0$ – for cohesive soils and $0 \leq \alpha \leq \phi$ – for the loose soil– like in the paper). The author took into consideration a dilation angle $\alpha = 5°$, cohesion and initial tension equal to 0 Pa. Furthermore, application of the Drucker-Prager model required determining the size of soil reinforcement. The reason for that was the elimination of the effect of cohesion on the soil behaviour. For this purpose, a parameter describing the soil reinforcement in compression was used, by fixing its size to 5 MPa. It should also be noted that the applied backfill types were not realistic (some of the parameters did not comply with others). The applied soils were in some sense the "theoretical soils", which can be created using cement, fibres, the variable of saturation degree, etc. The motivation of use of such types of soil was to estimate the impact of individual parameters on the behaviour of soil-steel composite culverts. Of course from the practical point of view, the applied backfills are not possible to use in the real soil-steel culverts. However, such analysis shows the impact of chosen parameters on the behaviour of CSP culverts.

– Road structure (crushed stone) with thickness of 0.36 m was defined as elastic-plastic material (solid-type element) with the hyperbolic Drucker-Prager yield criterion with unit weight $\gamma = 18.0$ kN/m^3, Young's modulus $E = 60$ MPa, angle of internal friction $f = 40°$, dilation angle $\alpha = 10°$, and initial tension 0 MPa. As in the case of basic backfill model, Drucker-Prager model-type reinforcement was applied, determining soil reinforcement parameter under compression equal to 5 MPa. Parameters of the substructure of crushed stone were the same in all analysed computational models of the culvert.

– Roadway layer (asphalt with thickness of 0.14 m) was modelled as an elastic material (solid-type element) with unit weight $\gamma = 21.0$ kN/m^3, Young›s modulus $E = 6.9$ GPa and Poisson›s ratio $\nu = 0.41$. Parameters of asphalt roadway were the same in all analysed computational models of the culvert.

– Boundary conditions: the author applied the total restraint, namely rotations and displacements along each axis of the shell's sides and base were blocked. In modelling, the CSP culvert was as a structure firmly embedded in the environment.

– Calculation step followed as $T = t + \Delta t$, where t is the initial time equal to $t = 0$ s, while Δt is time increment, during which the set static live load was applied, according to the three schemas used during experimental tests (Manko, Beben 2005). Accordingly, Δt equalled to the time in which load is applied, and the author adopted the value of 1 s. In calculation step ($T = 1$ s), successive iterations for increments caused by the load were made at that time. The author computed their effect on the CSP culvert behaviour using the software. Thus it was necessary to define the calculation step, the assumption of geometric non-linearity of the culvert (also specified in material characteristics of various components of the structure, i.e. soil and steel shell), which had a substantial effect on deformations occurring in the structure, caused by the applied forces. Beben, Stryczek (2016) considered similar assumptions.

3.3. Properties of contact elements

CSP culverts modelling consisting of three different layers (roadway elements (crushed stone and asphalt), backfill, CSP shell elements) with various physical properties required determination of their interactions. It is essential to determine these interactions among all layers, which were in direct contact, even if any of these have similar physical properties (backfill-crushed stone). For modelling interactions between different materials in the culvert, the author applied the contact elements, also called interfaces.

Interactions of materials such as steel shell-backfill, backfill-crushed stone, crushed stone-asphalt were modelled as rigid elements of the beam transferring their specific types of interactions from master to slave surfaces. These items included the phenomena occurring at the time of interaction between two materials, that was normal forces (rigidity) and friction forces (friction coefficient). Furthermore, Abaqus software allowed specifying the nature of surface interactions by defining the type of slide between contacting surfaces. Due to the nature of construction and behaviour of the entire culvert, which transferred loads to the last of its layers, that was corrugated plate, the type of interaction that occurred between the layers (asphalt-crushed stone, crushed stone-backfill) was defined as "finite sliding", which meant "not sliding". The basic argument for the establishment of this type of interaction was the fact that only in the last contact layer (CSP shell-backfill) small sliding of backfill surrounded by steel plate can occur. In this case, the author adopted an interaction in which "small sliding" was present.

The dependency of master and slave contact surfaces were determined based on the modulus of elasticity of materials being in touch with each other (interaction) and the nature of the CSP culvert behaviour. Slave was a surface build of the material with a lower modulus of elasticity (Young's modulus), and the surface with a higher modulus of elasticity represented a master. In numerical model, the author identified three types of contact areas (asphalt–crushed stone, crushed stone-backfill and backfill-CSP). For individual layers, following master-slave dependencies were adopted, that is: (a) asphalt – crushed stone → slave – master; (b) crushed stone – backfill → slave –master; (c) backfill – CSP shell→ slave – master.

The type of surface, being in contact with one another was the basis for determining two types of interaction properties specifying friction coefficients between the layers, and surface rigidity formed by these layers. Selecting these two types of interaction properties was the result of specific nature of backfill-CSP shell interaction, compared with other contact surface properties with relatively similar characteristics (asphalt–crushed stone, crushed stone-backfill). The crucial element, distinguishing this type of

interactions from others, was the smooth surface of the shell, which implies lower friction coefficient. Therefore, following friction coefficients were adopted: for backfill-CSP shell contact surface in the value of 0.3 and for other surfaces of 0.6. However, connection rigidity was established at the level of 2000 GN/m – for backfill-CSP shell contact surface and 2 GN/m – for other surfaces.

4. 3D analysis of the culvert

4.1. Applied schemes of live loads

During numerical calculations, the author used the same loads (real forces coming from the vehicle with a weight of 255 kN), which Manko, Beben (2005) applied during the experimental study of a culvert under static live loads. Table 3 shows the pressure on axles and wheels of the vehicle.

Table 3. Technical characteristics of the load distribution of the vehicle used for experimental studies and numerical calculations

Total weight, kN	Pressure on axles, kN		Pressure on wheels, kN	
	rear	front	rear	front
255.00	178 = 2·89.00	70.70	44.50	35.35

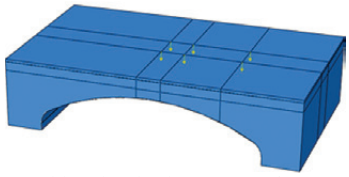

Fig. 4. Symmetrical live load scheme (B) of CSP culvert

To directly compare calculation results with experimental ones, three live load schemes were used in the numerical analysis (A, B and C) that correspond to those employed in the experimental studies:

– Scheme A (asymmetrical) – vehicle was positioned at a distance of 0.75 m from the left edge of the road, parallel to the longitudinal axis of the object. The rear axles of the vehicle were located over the crown (centre span) of the culvert.

– Scheme B (symmetrical) – vehicle was positioned in the middle of the road; its axle coincided with the longitudinal axis of the object. The rear axles of the vehicle were located over the crown (centre span) of the culvert (Fig. 4).

– Scheme C (asymmetrical) – the loading vehicle arranged as in Scheme A, only at the second edge of the culvert roadway.

4.2. Results of numerical calculations

The maps of displacements and stresses allowed to present the results of numerical calculations (Figs 5, 6 and 7). Maximum displacement values were 3.02 mm. These values appeared in the shell crown of a culvert for numerical model III (static live-load scheme C). In the case of numerical models I and II (load scheme C), the maximum

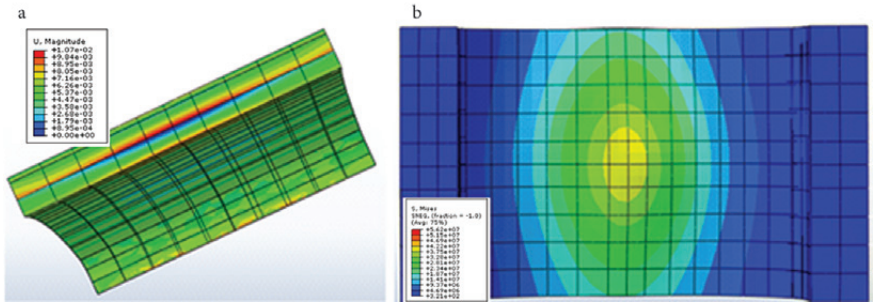

Fig. 5. Calculation results from live-load scheme A for numerical model I: a – displacements distribution; b – stresses in culvert shell

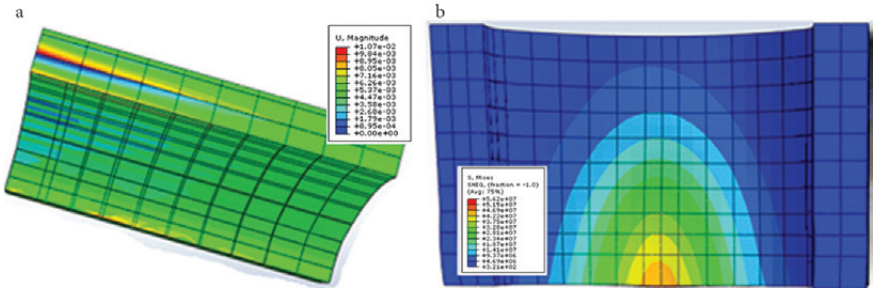

Fig. 6. Calculation results from live-load scheme B for numerical model II: a – displacements distribution; b –stresses in culvert shell

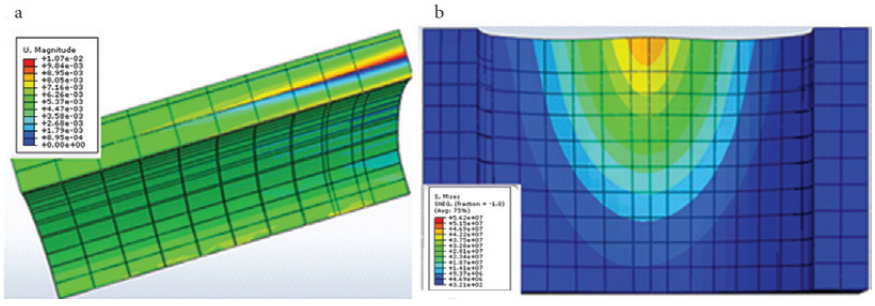

Fig. 7. Calculation results from live-load scheme C for numerical model III: a – displacements distribution; b – stresses in culvert shell

displacements of CSP culvert were equal to 2.91 mm and 2.59 mm, respectively. Maximum displacements occurred at the location where the load from the rear wheels of the vehicle were applied (in those places there were much greater displacements than in other parts of the bridge structures). In load schemes A and B, the largest displacements of the culvert also occurred for the numerical model III.

Maximum stresses (about 10.3 MPa), as in the case of displacements, were obtained for the numerical model III from the static live-load scheme A and C. In numerical models I and II, the highest stresses in the steel shell of the culvert amounted to 9.88 MPa and 9.03 MPa, respectively. Maps of stresses showed clearly that the greatest values appeared in application points of rear wheels (axes) of the loading vehicle, i.e. in the shell crown of the culvert. Similar findings appeared in the results of experimental studies presented by Manko, Beben (2005).

4.3. Analysis and discussion of results

Figures 8 and 9 showed the comparison of the calculated displacements and stresses for particular numerical models (types of backfills). Figures also showed the course of the experimental curves (maximum displacements and stresses). One can also observe the impact of backfills used to the effort of the steel shell.

As visible in Fig. 8, the calculated displacements of CSP culvert with the use of Abaqus program for three types of backfills were similar to each other (shape of the curves was similar). However, they were higher than the measured values. It is an evidence of the similar behaviour of structure and method of distributing loads by different but similar backfill parameters. The author noted that the maximum displacement from the experimental studies occurred at other points than in the case of numerical calculations. These differences indicate some heterogeneity in the actual culvert, e.g. in the backfill and at the joints of sheets of corrugated plates (possible gaps). Additionally, in numerical calculations, the existence of a uniform backfill and no connections between the sheets have been assumed. Relative differences between calculated and measured displacements for different numerical models were in the range: I (18–43%), II (1–36%) and III (30–45%). It is important to note that the best compliance of calculated and measured values occurred for numerical model II and live load scheme B.

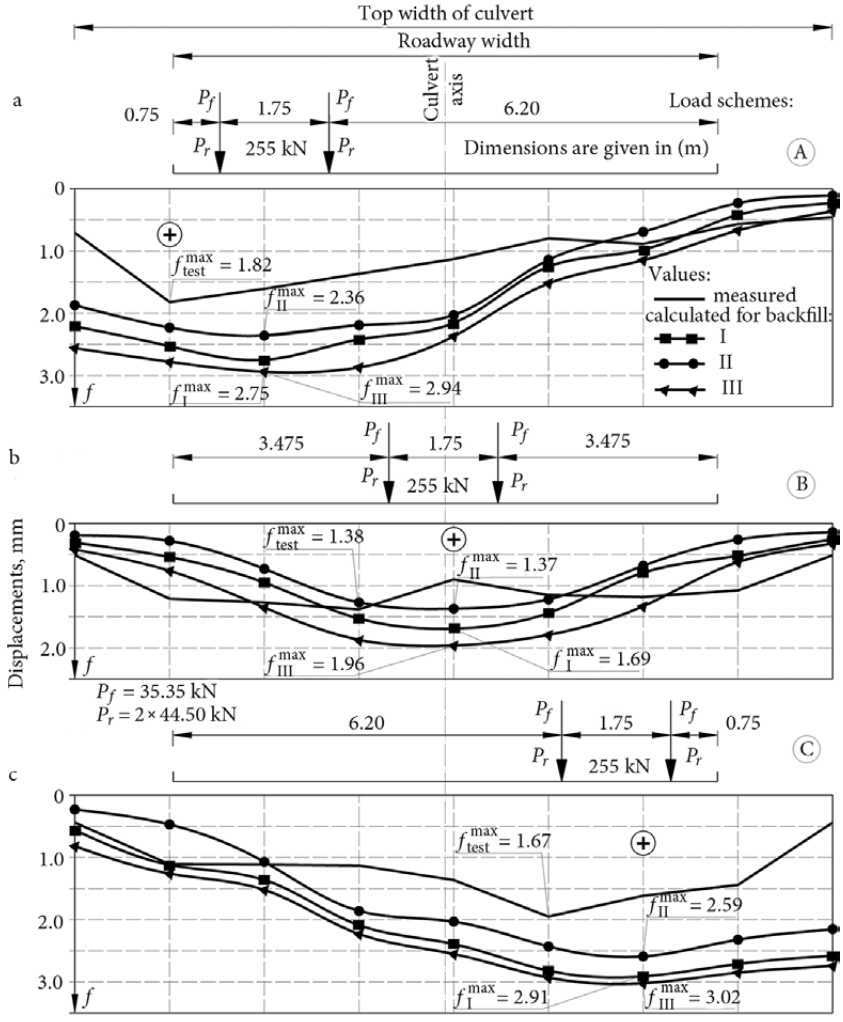

Fig. 8. Displacement courses at the culvert crown for three-backfill types and three static live-load schemes

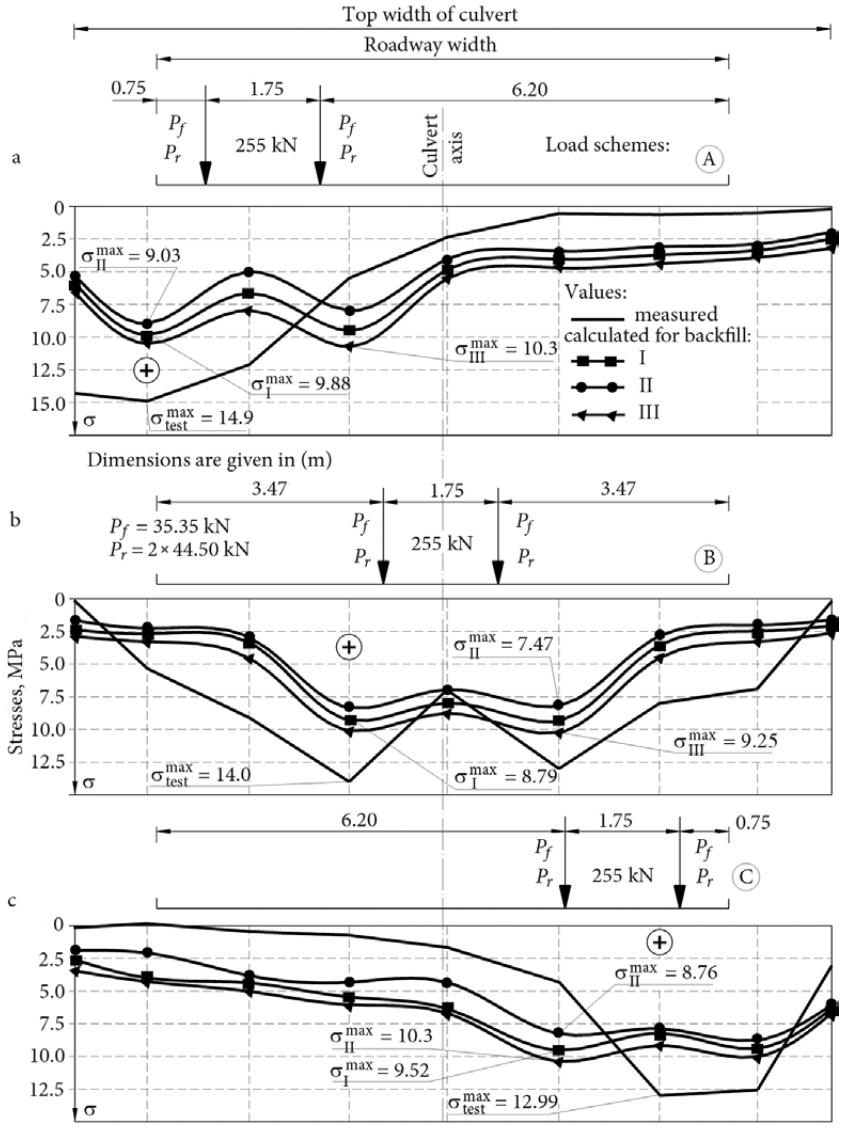

Fig. 9. Stresses courses at the crown of culvert shell for three backfill types and three static live-load schemes

Results and shape of displacement curves from live load schemes A and C were similar. In the case of load scheme B (vehicle positioned in the centre of the road) much smaller displacement values can be observed (54–89%) than for schemes A and C (despite the used of the same loading vehicle). In this case, the author noted that the course of displacements was uniform across the width of the culvert (no sudden leaps of value). Behaviour of the CSP culvert caused by the schemes A and C clearly show that side parts of the shell structure of the culvert have much higher deformations than in case of effect of a vehicle positioned according to the load scheme B. This indicates the lower rigidity and interaction backfill-shell at the ends of the culvert, and at the same time, a better load distribution in the soil in the middle of the culvert (load scheme B). Therefore, it seemed logical and justified to use additional reinforcements at the beginning and end of the culvert. The most similar values of calculated displacements to the measured appeared with the use of numerical model II. Thus, the relative differences of calculated displacements with the use of numerical models I and III versus the model II were accordingly in the range (11–23%) and (14–30%).

Figure 9 showed values of stresses in characteristic points of the structure (for which the author also made measurements previously) for three types of backfill calculated in Abaqus program. In this case, the influence of backfill parameters on the effort of the shell of CSP culvert was also visible (similar shapes of courses). It was noted especially that maximum calculated stresses in the culvert shell crown were smaller than the measured values, but it should be also pointed that the width of the culvert – *y*-axis (beyond the immediate range of the load action) measured values were lower than the calculated ones (particularly for scheme A and load C – Figs 8 and 9). The greatest stresses occurred directly beneath the real forces constituting pressures of the tires. Fig. 9 also showed that the maximum stresses occurred from asymmetrical live-load schemes A and C. This may result from some heterogeneity and lower

rigidity at the ends of the culvert (similar tendencies were achived in the case of displacements). Furthermore, it was visible that vehicle position according to the scheme B (in the middle of the road) resulted in a rather uniform load distribution, what indicated the involvement of a greater width of the CSP culvert into interaction in the transfer of a given live load.

Additionally, one can observe (as in the case of displacements) that the distribution of calculated stresses was gentler (no sharp bends) than in the case of measured values. Relative differences between calculated and measured stresses for different numerical models were in the range: I (27–37%), II (33–47%) and III (21–34%). The most similar values of calculated stresses to the measured appeared with the use of numerical model III (for maximum values). However, taking the entire width of the culvert into account (Fig. 9), the numerical model II proved to be the most favourable. Thus, the relative differences of calculated stresses with the use of numerical models I and III versus the model II were accordingly in the range (8–15%) and (12–19%) for the benefit of model II.

The smallest displacements and stresses in the shell of CSP culvert were obtained for the numerical model II (Fig. 10). In this model, the backfill parameters were as follows: angle of internal friction 40°, unit weight 18 kN/m^3 and Young's modulus 70 MPa. The author noted that among the selected parameters of backfills in all analysed numerical models, the angle of internal friction seems to have the greatest influence on the size of displacements and stresses of the culvert. It indicates that for the considered parameter ranges of backfill, the effect of Young's modulus was not a key parameter to reduce the deformation of the culvert. Besides, the author conducted additional numerical calculations concerning the impact of Young's modulus on deformation of the CSP culvert. The Young's modulus (70 MPa like in the second model) for numerical models I and III were used. The obtained results did not vary more than 3% against previous numerical calculations. However, one can assume that there is a limit of Young's modulus values, below which deformations of the culvert would increase significantly. Similarly, to Young's modulus parameterization, unit weight of soil (18 kN/m^3) was applied for numerical models I and III. In this case, the obtained results did not also vary more than 3–5% versus previous calculations. It also follows that the compaction degree of backfill (directly dependent on the angle of internal friction) was an important parameter. Although for the angle of internal friction equal to 45° the smallest values were not obtained, at the value of 35° the greatest deformations of the culvert have been noted. In addition, the author noted that the angle of internal friction is a parameter of shear strength of the soil. The author also observed that, together with decreasing of the angle of internal friction and increasing the unit weight and Young's modulus of the backfill (Table 2) displacement and stress of the culvert increased. Increasing Young's modulus and unit weight of the backfill in numerical models did not reduce the deformation of the culvert.

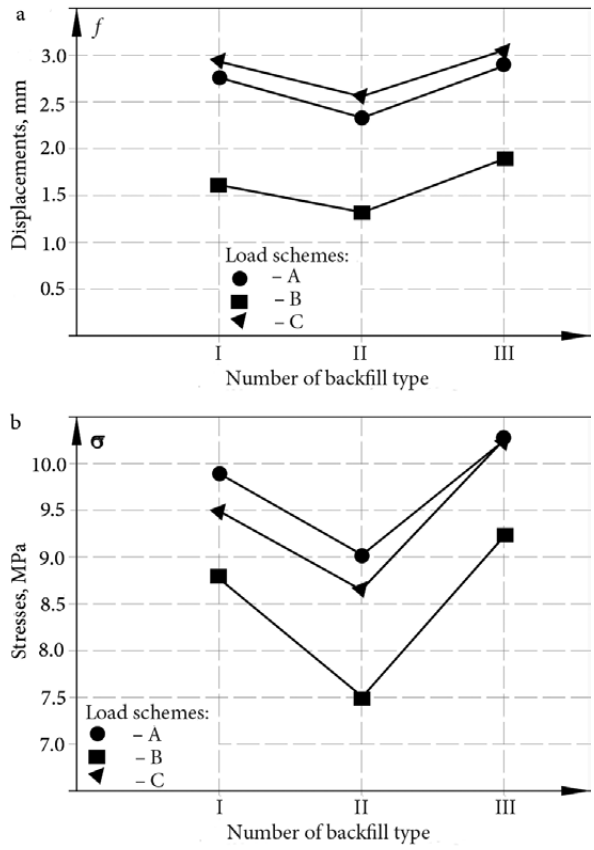

Fig. 10. Maximum displacements (a) and stresses (b) of culvert shell for three-backfill type and three static live-load schemes

New numerical simulations for a larger range of parameters of backfill seem to be desired in order to draw a more detailed dependence of impact of backfill quality to deformation of this type of bridge. It is hard to conclude that a parameter has a decisive influence on the level of deformation of CSP culvert because they are directly interrelated. In summary, taking into consideration the relatively small range of variability of backfill parameters, it seems that the angle of internal friction plays a key role in the behaviour of CSP culvert.

5. Conclusions

As a result of numerical calculations of CSP culvert for selected "theoretical" types of backfills and comparison of these results with experimental values, the following conclusions can be drawn out:

1. The quality of backfills was a major factor during the design of CSP culverts. Backfills used in the computational analysis, although they were different regarding parameters, distributed the loads in a similar way, as evidenced by the similar shapes of graphs.

2. Parametric analysis showed that the angle of internal friction was a major factor in CSP culverts. The greatest deformations of culvert appeared for the smallest internal friction angle (35°). The author noted that particularly when the unit weight increased and the angle of internal friction decreased, deformation in a steel shell also

increased. Increasing Young's modulus of the backfill did not reduce the deformation of the culvert.

3. Considering the entire width of the CSP culvert, the calculation model II was most favourable. Relative differences of the obtained values with the use of models I and III versus the model II were accordingly in the range (8–15%) and (12–19%) for stresses and (11–23%) and (14–30%) for displacements for the benefit of model II.

4. Calculated displacements were higher than measured (taking the entire width of the culvert into account), and the maximum calculated stresses were smaller than in the experiments. It can be a result of the increased rigidity of calculation models of the analysed culvert than is apparent from its actual structure (e.g. the occurrence of gaps at the junctions of steel sheets and heterogeneity in the backfill). However, taking the entire width of the culvert into account (the area outside the immediate range of the load acting), measured stresses were less than the calculated (especially for live-load scheme A and C).

5. Maximum stresses (10.3 MPa) and displacements (3.02 mm) from numerical calculations occurred in the shell crown of culvert from asymmetrical live-load schemes A and C. This showed lower rigidity and interaction backfill-shell at the ends of the culvert. Furthermore, one can observe that the position of the vehicle with the same weight according to the scheme B (in the middle of the road) resulted in a rather uniform load distribution. It indicated the involvement of a greater width of the CSP culvert into interaction in the transfer of a given live load.

6. The proposed method of modelling of the CSP culvert allowed obtaining reasonable values of displacements and stresses in comparison to experimental results and analytical methods. However, to provide detailed recommendations for the impact of backfill condition, further parametric studies are required, especially for wider backfill parameters. It would be better to focus on one parameter at each stage of calculations for a deeper and a meaningful comparison.

References

Beben, D.; Stryczek, A. 2016. Numerical Analysis of Corrugated Steel Plate Bridge with Reinforced Concrete Relieving Slab, *Journal of Civil Engineering and Management* 22(5): 585–596. https://doi.org/10.3846/13923730.2014.914092

Beben, D. 2014. Corrugated Steel Plate (CSP) Culvert Response to Service Train Loads, *Journal of Performance of Constructed Facilities* 28(2): 376–390. https://doi.org/10.1061/(ASCE)CF.1943-5509.0000422

Beben, D. 2013a. Experimental Study on Dynamic Impacts of Service Train Loads on a Corrugated Steel Plate Culvert, *Journal of Bridge Engineering* 18(4): 339–346. https://doi.org/10.1061/(ASCE)BE.1943-5592.0000395

Beben, D. 2013b. Field Performance of Corrugated Steel Plate Road Culvert under Normal Live Load Conditions, *Journal of Performance of Constructed Facilities* 27(6): 807–817. https://doi.org/10.1061/(ASCE)CF.1943-5509.0000389

Brachman, R.; Elshimi, T.; Mak, A.; Moore, I. 2012. Testing and Analysis of a Deep-Corrugated Large-Span Box Culvert Prior to Burial, *Journal of Bridge Engineering* 17(1): 81–88. https://doi.org/10.1061/(ASCE)BE.1943-5592.0000202

Elshimi, T. M.; Brachman, R. W. I.; Moore, I. D. 2014. Effect of Truck Position and Multiple Truck Loading on Response of Long-Span Metal Culverts, *Canadian Geotechnical Journal* 51(2): 196–207. https://doi.org/10.1139/cgj-2013-0176

El-Taher, M. 2009. *The Effect of Wall and Backfill Soil Deterioration on Corrugated Metal Culvert Stability*: Dissertation, Queen's University.

Esmaeili, M.; Zakeri, J. A.; Abdulrazagh, P. H. 2013. Minimum Depth of Soil Cover above Long-Span Soil-Steel Railway Bridges, *International Journal of Advanced Structural Engineering* 5: 7. https://doi.org/10.1186/2008-6695-5-7

Flener, B. E. 2010. Testing the Response of Box-Type Soil-Steel Structures under Static Service Loads, *Journal of Bridge Engineering* 15(1): 90–97. https://doi.org/10.1061/(ASCE)BE.1943-5592.0000041

Flener, B. E. 2009a. Response of Long-Span Box Type Soil-Steel Composite Structures during Ultimate Loading Tests, *Journal of Bridge Engineering* 14(6): 496–506. https://doi.org/10.1061/(ASCE)BE.1943-5592.0000031

Flener, E. B.; Karoumi, R. 2009b. Dynamic Testing of a Soil-Steel Composite Railway Bridge, *Engineering Structures* 31(12): 2803–2811. https://doi.org/10.1016/j.engstruct.2009.07.028

Janusz, L.; Madaj, A. 2009. *Engineering Structures from Corrugated Plates. Design and Construction.* Transport and Communication Publishers, Warsaw, Poland, 427 p.

Katona, M. G. 2010. Seismic Design and Analysis of Buried Culverts and Structures, *Journal of Pipeline Systems Engineering and Practice* 1(3): 111–119. https://doi.org/10.1061/(ASCE)PS.1949-1204.0000057

Kunecki, B. 2006. Full-Scale Test of Corrugated Steel Culvert and FEM Analysis with Various Static Systems, *Studia Geotechnica et Mechanica* 28(2–4): 39–54.

Machelski, C. 2008. *Modeling of Soil-Shell Bridge Structures.* The Lower Silesian Educational Publishers, Wroclaw, Poland, 205 p.

Mai, V. T.; Hoult, N. A.; Moore, I. D. 2014a. Effect of Deterioration on the Performance of Corrugated Steel Culverts, *Journal of Geotechnical and Geoenvironmental Engineering* 140(2). https://doi.org/10.1061/(ASCE)GT.1943-5606.0001021

Mai, V. T.; Moore, I. D.; Hoult, N. A. 2014b. Performance of Two-Dimensional Analysis: Deteriorated Metal Culverts under Surface Live Load, *Tunneling and Underground Space Technology* 42: 152–160. https://doi.org/10.1016/j.tust.2014.02.015

Manko, Z.; Beben, D. 2005. Static Load Tests of a Road Bridge with a Flexible Structure Made from Super Cor Type Steel Corrugated Plates, *Journal of Bridge Engineering* 10(5): 604–621. https://doi.org/10.1061/(ASCE)1084-0702(2005)10:5(604)

Mellat, P.; Andersson, A.; Pettersson, L.; Karoumi, R. 2014. Dynamic Behaviour of a Short Span Soil–Steel Composite Bridge for High-Speed Railways – Field Measurements and FE-Analysis, *Engineering Structures* 69: 49–61. https://doi.org/10.1016/j.engstruct.2014.03.004

Pettersson, L.; Flener, E. B.; Sundquist, H. 2015. Design of Soil–Steel Composite Bridges, *Structural Engineering International* 25(2): 159–172. https://doi.org/10.2749/101686614X14043795570499

Pettersson, L.; Sundquist, H. 2014. *Design of Soil Steel Composite Bridges*. 5th edition. TRITA-BKN, Stockholm, Sweden, 98 p.

Sargand, S.; Masada, T.; Moreland, A. 2008. Measured Field Performance and Computer Analysis of Large-Diameter Multi-Plate Steel Pipe Culvert Installed in Ohio, *Journal of Performance of Constructed Facilities* 22(6): 391–397. https://doi.org/10.1061/(ASCE)0887-3828(2008)22:6(391)

Sezen, H.; Yeau, K. Y.; Fox, P. J. 2008. In-Situ Load Testing of Corrugated Steel Pipe-Arch Culverts, *Journal of Performance of Constructed Facilities* 22(4): 245–252. https://doi.org/10.1061/(ASCE)0887-3828(2008)22:4(245)

Sheldon, T.; Sezen, H.; Moore, I. D. 2015. Joint Response of Existing Pipe Culverts under Surface Live Loads, *Journal of Performance of Constructed Facilities* 29(1). https://doi.org/10.1061/(ASCE)CF.1943-5509.0000494

Simpson, B.; Moore, I. D.; Hoult, N. A. 2015. Experimental Investigation of Rehabilitated Steel Culvert Performance under Static Surface Loading, *Journal of Geotechnical and Geoenvironmental Engineering* 142(2). https://doi.org/10.1061/(ASCE)GT.1943-5606.0001406

Wadi, A.; Pettersson, L.; Karoumi, R. 2015. Flexible Culverts in Sloping Terrain: Numerical Simulation of Soil Loading Effects, *Engineering Structures* 101: 111–124. https://doi.org/10.1016/j.engstruct.2015.07.004

Yeau, K. Y.; Sezen, H.; Fox, P. J. 2014. Simulation of Behavior of in-Service Metal Culverts, *Journal of Pipeline Systems Engineering and Practice* 5(2). https://doi.org/10.1061/(ASCE)PS.1949-1204.0000158

Yeau, K. Y.; Sezen, H. 2012. Load-Rating Procedures and Performance Evaluation of Metal Culverts, *Journal of Bridge Engineering* 17(1): 71–80. https://doi.org/10.1061/(ASCE)BE.1943-5592.0000213

Yeau, K. Y.; Sezen, H.; Fox, P. J. 2009. Load Performance of in Situ Corrugated Steel Highway Culverts, *Journal of Performance of Constructed Facilities* 23(1): 32–39. https://doi.org/10.1061/(ASCE)0887-3828(2009)23:1(32)

Zienkiewicz, O. C.; Taylor, R. L. 2000. *Finite Element Method. Volume 2: Solid Mechanics*. Butterworth-Heinemann, Oxford, 459 p.

Received 3 November 2015; accepted 2 January 2017